Title	Comprehensive analysis of step-feeding strategy to enhance biological nitrogen removal in alum sludge-based tidal flow constructed wetlands
Authors(s)	Hu, Y.S., Zhao, Y.Q., Zhao, X.H., Kumar, J.L.G.
Publication date	2012-05
Publication information	Hu, Y.S., Y.Q. Zhao, X.H. Zhao, and J.L.G. Kumar. “Comprehensive Analysis of Step-Feeding Strategy to Enhance Biological Nitrogen Removal in Alum Sludge-Based Tidal Flow Constructed Wetlands.” Elsevier, May 2012. https://doi.org/10.1016/j.biortech.2012.01.165.
Publisher	Elsevier
Item record/more information	http://hdl.handle.net/10197/4021
Publisher's statement	This is the author’s version of a work that was accepted for publication in Bioresource Technology resulting from the publishing process, such as peer review, editing, corrections, structural formatting, and other quality control mechanisms may not be reflected in this document. Changes may have been made to this work since it was submitted for publication. A definitive version was subsequently published in Bioresource Technology (Volume 111, May 2012, Pages 27–35) DOI:# 10.1016/j.biortech.2012.01.165 Elsevier Ltd.
Publisher's version (DOI)	10.1016/j.biortech.2012.01.165

Comprehensive analysis of step-feeding strategy to enhance biological nitrogen removal in alum sludge-based tidal flow constructed wetlands

Y.S. Hu, Y.Q. Zhao*, X.H. Zhao, J.L.G. Kumar

Centre for Water Resources Research, School of Civil, Structural and Environmental Engineering, University College Dublin, Newstead Building, Belfield, Dublin 4, Ireland

*Corresponding author: Tel +353-1-7163215; Fax +353-1-7163297; E-mail yaqian.zhao@ucd.ie

Abstract: Step-feeding strategies have been extensively studied and comprehensively analyzed in this study for a four-stage alum sludge-based tidal flow constructed wetlands (AlS-TFCWs) system. Enhanced total nitrogen removal of 83% is achieved under high nitrogen loading rate of 19.1 g N/m^2 d. The key issues towards the success of a significant nitrogen removal in step-feeding TFCWs are the bed resting time (which provides better aeration for nitrification) and up flow stage/delayed input of side stream(s) (which ensure favorable environment for better denitrification). Simultaneous nitrification and denitrification (SND) was found effective in the 1st stage of the system and SND via nitrite is the main nitrogen conversion mechanism. The optimal influent distribution fraction for

step-feeding purpose can be estimated from a theoretical basis, which is a function of the influent BCOD/TKN ratio. Therefore the influent distribution fraction should be adjusted according to the variety of influent characteristics, rather than a fixed value.

Keywords: Alum sludge, partial nitrification, simultaneous nitrification and denitrification (SND), step-feeding, tidal flow constructed wetlands

1. Introduction

'Tidal flow' constructed wetlands (TFCWs) is one of the most significant developments in treatment wetlands in the last ten years (Chan et al., 2008; Sun et al., 1999a , 1999b, 2006; Zhao et al., 2004a, 2004b). The key features of TFCWs are batch pulse feeding and alternant saturation/unsaturation of the wetland medium with wastewater. By this way, oxygen transfer is greatly enhanced and the treatment capacity is then significantly improved. In practice, it is usually configured in multiple stages by connecting several identical wetland stages in series (Zhao et al., 2004a). Wastewater is batch loaded to the first stage and sequentially passes through the rest, generating periodic wet/dry period in individual stages. More significantly, a so-called alum sludge-based TFCWs (AlS-TFCWs), which adopts dewatered alum sludge (DAS) as the main wetland medium, has been developed and demonstrated to have excellent capability in organic matter (OM), ammoniacal nitrogen (NH_4^+-N) and phosphorus (P) removal (Zhao et al., 2011; 2009). It is fair to note that such the development represents a novel approach in treatment wetland technology. In a previous pilot-scale four stages AlS-TFCWs study, NH_4^+-N removal efficiency up to 98% and mean monthly removal efficiency above 85% were recorded under various loading rate from 7.1 to 47 g N/m^2 d. However, total nitrogen (TN) removal was still not desirable with monthly mean removal efficiency of 11-78% (Zhao et al., 2011). Analysis of nitrogen profiles in individual stages revealed that the influent carbon source was almost depleted in the first 3 stages before full nitrification was completed (Zhao et al., 2011). Consequently, denitrification was getting limited along the stages, resulting in high nitrified effluent and limited TN reduction. Hence, modification of the original TFCWs configuration is necessary in order to achieve satisfactory TN removal performance.

Step-feeding has been broadly demonstrated in conventional activated sludge (AS) process as an effective option to enhance TN removal by stepwise introduction of the influent to the nitrified liquid, thus making more efficient use of the influent carbon source for denitrification (Fillos et al., 1996; Fujii, 1996; Liang et al., 2010; Puig et al., 2004; Tang et al., 2007). Although this setup has been adopted in some constructed wetlands (CWs) systems, the main purpose lies in the effective utilization of wetland area through uniform loading distribution (Dialynas et al., 2002; Reed and Brown, 1992; Sundaravadivel and Vigneswaran, 2001). Only few studies in CWs valued its role in enhancing denitrification (House et al., 1999; Stefanakis et al., 2011; Yang et al., 2011). In this study, step-feeding was adopted as the key strategy aimed to enhance the TN removal performance for a four stages AlS-TFCWs. Effects of different step-feeding schemes and operational conditions on the treatment performance are comprehensively evaluated. Diversity of nitrifying activities and nitrogen removal pathway in different stages is investigated in detail. Finally, optimal configuration of step-feeding AlS-TFCWs is proposed and analyzed for maximum nitrogen removal.

2. Materials and method

2.1 System description and operation

The laboratory scale four stages AlS-TFCWs system was constructed with four identical plexiglass columns connected in series (Fig. 1) and operated under room temperature. 10 cm-depth gravel was filled into the bottom as the support media. Air-dried DAS (2 kg for each stage, moisture content 74%, particle size 1-3 cm) collected from a local water treatment plant, was filled as the main medium layer. It has been determined in previous study that the DAS was mainly composed of amorphous aluminium, and more importantly, the DAS exhibited a high phosphorus (P) adsorption capacity of 31.9 mg P/g DAS (Babatunde et al., 2009). The total volume of each stage was 4.75 L with a working volume of 2 L (initial porosity of 42%). Common reeds, *Phragmites australis,* were planted on the top. Each stage experienced cyclic 'Wet/Dry' periods with the 'tides' of wastewater generated by peristaltic pumps, which were controlled by pre-set programmable timers. The system was inoculated with activated sludge obtained from a local municipal wastewater treatment plant for 3 weeks. Thereafter, four step-feeding schemes (marked as A to D) were tested with different input points, distribution ratios, main flow patterns and cycle duration (T_C), as shown in Fig. 1 and summarized in Table 1. In all the schemes, there was a primary feed (80-90% of the overall flow rate) introduced into stage 1 (Feed 1). The rest fraction of the influent was then distributed into stage 3 (Feed 2) and/or stage 4 (Feed 3). Side stream

(Feed 2/Feed 3) was introduced into side input point in synchronization with the main flow in period A and B, while it was delayed for 2 hrs after the main flow in period C and D.

[Fig. 1]

[Table 1]

2.2 Wastewater

Piggery wastewater was used as the influent source. The raw wastewater was collected from an animal farm at Newcastle, Co. Dublin, Ireland. After collection, it was diluted with tap water to obtain desired strength and served as the influent. The influent wastewater characteristics and loading rates during each step-feeding scheme were summarized in Table 2.

[Table 2]

2.3 Mass balances

In order to explore the characteristics of nitrogen removal in individual stages under different operational conditions, contributions of each stage to the overall nitrogen removal were estimated by mass balancing. The net mass flux of NH_4^+-N reduction ($\varphi_{NH4,Re.}$) and

NO_X^--N (NO_2^--N + NO_3^--N) accumulation ($\varphi_{NOX,Acc.}$) in each stage were calculated according to Table 3. The calculation was based on the simplifying assumption that NH_4^+-N reduction was due to nitrification, thus the nitrogen loss by biomass assimilation and plant uptake was neglectable (Stottmeister et al., 2003). The negative value for $\varphi_{NH4, Re.}$ implies that the amount of NH_4^+-N produced via ammonification exceeds the amount of NH_4^+-N reduced due to nitrification. Accordingly, the negative value for $\varphi_{NOX, Acc.}$ suggests that the amount of NO_X^--N removed via denitrification is above the amount of NO_X^--N produced through nitrification. The removal percentage of the influent NH_4^+-N in each stage was calculated as the $\varphi_{NH4, Re.}$ of each stage divided by the influent NH_4^+-N loading.

[Table 3]

2.4 Microbial activities

Microbial activities of heterotrophic biomass (X_H) and autotrophic biomass (ammonia oxidization bacteria, AOB; nitrite oxidization bacteria, NOB) in each stage were assessed by oxygen uptake rate (OUR) test (Ginestet et al., 1998) at the end of scheme D. Respiration measurements were carried out with a fed batch respirometer (V=280 mL) at room temperature (23 ±0.5 ℃). Representative DAS samples were obtained from each stage by mixing the medium of the whole bed. All the samples were washed several times with distilled water one day before the tests to remove the residual substrates. Thereafter, predetermined amount of the prepared DAS sample was grounded and introduced into the respirometer. The respirometer was then filled up with distilled water together with nutrient buffer (Sato et al., 1985). The mixed liquid was aerated until saturation before the respirometer was carefully closed and was then keeping stirred by a magnetic stirrer at 250 rpm. Dissolved oxygen (DO) was recorded every 30s during a subsequent addition of substrates and selective inhibitors - Allylthiourea (ATU) for AOB and Azide for NOB from an injection port. The whole procedure lasted between 20 to 40 minutes. The OUR was determined by linear regression and expressed as mg O_2/L of DAS h. Samples were prepared in duplicate.

2.5 Sampling and chemical analyses

Grab samples from influent, effluent and the outflow of each stage were collected 1-2 times a week and analyzed for COD, BOD_5, TN, NO_2^--N, NO_3^--N, NH_4^+-N, TP, PO_4^{3-}-P, suspended solid (SS) and pH. COD, NH_4^+-N, NO_2^--N, NO_3^--N, PO_4^{3-}-P and SS were analyzed using a Hach DR/2400 spectrophotometer according to its standard operating procedures. BOD_5 was measured with a Hach BODTrak instrument. TP and TN were determined with ascorbic method and persulfate method respectively (Clesceri et al., 1998). pH was measured with a pH meter (Orion 920 A+, Thermo). DO was monitored with a microprocessor oximeter (Oxi 325, WTW).

2.6 Statistical analyses

In order to investigate the difference in treatment performance between different step-feeding schemes, statistical analyses were carried out using PASW Statistics 18 (SPSS Inc.). One way ANOVA multiple comparisons for the mean removal efficiencies were computed with Tamhane's T2 test at 95% confidence level (α=0.05). The method was selected for that equal variance between groups was not assumed.

3. Results and discussion

3.1 Overall performance

The overall performance of the AlS-TFCWs with different step-feeding schemes is illustrated in Fig. 2. The system demonstrated satisfactory performance in SS, OM, P and NH_4^+-N removal. Average SS removal was above 90% for all the tested schemes (Fig. 2a). With regard to OM, average COD removal above 80% was achieved in all the schemes except for scheme C (74%). Removal of BOD_5 was more effective and stable with mean removal efficiency of 85% for scheme A and above 90% for the rest schemes (Fig. 2b). This indicates that the system can substantially remove the biodegradable part of the influent organic carbon. Fig. 2c illustrates efficient and stable TP elimination regardless of the operational conditions. Average TP removal efficiency still remained above 95% in scheme D after 383 days operation under high PLR of 2.9-4.0 g P/m^2 d.

Average NH_4^+-N removal was 88%, 97%, 93% and 96% for scheme A, B, C and D, respectively (Fig. 2d), indicating that the nitrification was not the limiting step for effective TN removal (>80%). Instead, TN removal was limited by denitrification (Fig. 2e, f). Only

61% TN removal was achieved in average with scheme A. It was followed by the increase to 72% and 70% with scheme B and C, respectively. The best performance in TN removal was obtained with scheme D with average of 83%, which was a substantial improvement compared with the general TN removal of 23-59% in the original TFCWs (Babatunde et al., 2010; Sun et al., 1999b; Sun et al., 2006; Sun et al., 2005). This demonstrates that step-feeding is an effective strategy for TFCWs to enhance TN removal performance.

[Fig. 2]

3.2 Multiple comparisons of different step-feeding schemes on treatment performance

Table 4 presents the results of multiple comparisons (One way ANOVA) on the mean removal efficiencies between different step-feeding schemes. There was no significant difference on SS removal between different schemes. For COD, mean removal efficiency with scheme C was significantly lower than scheme A and B by 8.7% and 9.9%, respectively. However, it is insufficient to draw the conclusion that there was significant difference in OM removal between different schemes, because there was no statistical difference on BOD_5 degradation. The difference in COD removal might be derived from the fact that the influent COD in scheme C contained higher inert fraction, which could not be removed biologically (Hu et al., 2011). As to TP, the mean removal efficiency with scheme D was slightly lower than scheme A by 2.7% probably due to the P saturation progress after long term operation. The nitrification performance with scheme A was significantly lower than scheme B, C and D by 9.6%, 5.1% and 8.7%, respectively. And the nitrification performance with scheme C was considerably lower than scheme B and D by 4.5% and 3.6%, respectively, while there was no statistical difference between scheme B and D. For TN, scheme D was significantly higher than scheme A, B and C by 22.2%, 11.1% and 13.3%, respectively. These results reveal that step-feeding schemes have significant impact on nitrogen removal, which deserves further analysis and discussion.

[Table 4]

3.3 Synergic effects of step-feeding, cycle duration and flow pattern on nitrogen removal

The cyclic nitrogen profiles under different schemes are illustrated in Fig. 3. It shows the impact of step-feeding on nitrogen removal characteristics in individual stages. For NH_4^+-N, major reduction occurred in stage 2 and 3 (58%) with scheme A, while it occurred in stage 1 and 2 with scheme B (72%), C (64%) and D (71%). Peak reduction took place in stage 3 for scheme A, stage 2 for scheme B and stage 1 for scheme C and D. It's very interesting to note that accumulation of NO_X^--N in stage 1 was always neglectable, which suggested that all the nitrified nitrogen was denitrified within this stage. This phenomenon is termed as simultaneous nitrification and denitrification (SND) (Münch et al., 1996; Pochana and Keller, 1999). The effective SND in stage 1 could be attributed to the facts that: 1) external carbon source was sufficient to support the full denitrification of the nitrified nitrogen; 2) anoxic condition was easily to be established due to rapid oxygen depletion caused by extensive OM oxidization and nitrification (Pochana and Keller, 1999). To take full advantage of this effect, appropriate step-feeding setup should be taken to make the NH_4^+-N reduction in the first stage as much as possible. Accordingly, scheme D seemed to meet this requirement best (Fig. 3). NO_X^--N accumulation started from stage 2 in all the schemes, which indicated that denitrification was limited due to carbon deficiency. This trend was reverted with the supplement of carbon source by wastewater step-feeding, which enabled denitrification to proceed again, resulting decrease of NO_X^--N in the side input stages (stage 4 in scheme B; stage 3 in scheme C and D) (Fig. 3).

[Fig. 3]

Fig. 4 shows the NH_4^+-N and NO_X^--N mass fluxes in each stage throughout the whole operation period, which further reveals the effects of step-feeding and operational conditions (T_C and main flow pattern) on nitrogen removal performance. Firstly, Fig. 4a and Fig. 4b reveal the impact of T_C and step-feeding on nitrification. The overall nitrification performance deteriorated seriously after around 100 days of operation with T_C of 4 hrs. Regarding individual stages, the deterioration only happened in the 1st stage, while nitrification in the following stages was actually enhanced due to the shift of the NH_4^+-N loading. Form day 102 to 122, the net NH_4^+-N reduction in stage 1 became negative (net NH_4^+-N production), which was derived from the completely inhibited nitrification and strong ammonification. To overcome this problem, T_C was then increased to 6 hrs from day 123. The reflection of this action was observed immediately on day 124 with the recovery of the overall nitrification performance. After that, nitrification in stage 1 was fully recovered and enhanced overall nitrification performance was maintained for the rest operation period of 259 days. This suggested that T_C of 6 hrs was necessary and sufficient to maintain long term stability of effective nitrification for the current loading. As listed in Table 1, the contact time (Wet) was actually more or less the same between the two cycle duration schemes. The difference was the bed resting time (Dry), which was only 10 minutes in T_C of 4 hrs while it increased to 120 minutes in T_C of 6 hrs. This strongly indicates that the bed resting plays the key role in nitrification. Similar result was reported by Zhao et al., (2004b) on observation of enhanced pollutants removal efficiencies with a relatively short contact time and long bed resting period. Besides bed resting, step-feeding was showed to have important impact on the nitrification characteristics as well. With the same T_C and contacting/resting time, NH_4^+-N reduction in stage 1 with scheme D was markedly higher than scheme B and C. This is of great significance for the overall TN removal by taking the advantage of SND in the 1st stage as discussed above.

Fig. 4c reveals the effects of step-feeding and main flow pattern on denitrification. The effectiveness of step-feeding can be observed with the reduced mass accumulation of NO_X^--N in the side input stages, such as stage 3 and 4 in scheme B and especially stage 3 in scheme C and D. As can be seen in scheme C and D, net NO_X^--N accumulation was negative in stage 3 most of the time, which indicated that not only the nitrified N in the current stage was fully denitrified, but also certain amount of NO_X^--N from the previous stage was reduced. However, such effect was rarely observed in scheme A and B. The main flow patterns may account for this difference. The main flow in scheme A and B was downward, while it was upward in scheme C and D (Fig. 1). It was presumed that down flow would enhance oxygen transfer into the bed and this hypothesis was justified with the DO distribution measurement (Fig. 4d). It shows that the DO level with down flow was significantly higher than up flow. More interestingly, DO was increased as a function of the travel distance with down flow, while it remained more or less constant with up flow. In the view of hydraulics, down flow might be close to turbulent flow so the mixing of wastewater and air is extensive. The longer the wastewater travels, the more oxygen is dissolved in the bulk liquid. While up flow might be close to laminar flow and the mixing is limited, thus DO remains more or less the same and is independent of the travel distance. Obviously, the weakened oxygen transfer with up flow in scheme C and D was conducive to form effective anoxic condition and favored denitrification. Furthermore, the delayed introduction (2 hrs after the main flow) of the side stream in scheme C and D may also play an important role in the enhancement of denitrification. The reason was that more strictly anoxic condition could be established after the first 2 hrs contact, so that the introduced carbon source in the side stream could be fully utilized for denitrification instead of direct oxidization.

[Fig. 4]

The above results reveal the rationale of the enhanced TN removal performance with step-feeding. Such the step-feeding leads to more effective utilization of the influent carbon source compared with the original TFCWs configurations. The extent of denitrification relies on both available carbon source and nitrified nitrogen (Artan and Orhon, 2005). In the original TFCWs, all the stages are under aerobic phase to a certain extent with the enhanced oxygen transfer (Vymazal, 2011). In such case, major part of the influent carbon sources are directly oxidized prior to the availability of nitrified nitrogen. Consequently, the system is vulnerable to carbon limited situation (Babatunde et al., 2010; Sun et al., 2006, 2005, 1999b; Zhao et al., 2011). By adopting step-feeding, the carbon source introduced by the side stream can meet the nitrified nitrogen produced in the previous stages. This part of carbon source is then utilized for denitrification, accordingly, overcoming the carbon deficiency problem in the original TFCWs and resulting in an enhanced TN elimination.

3.4 Microbial activities and nitrogen conversion pathway

Fig. 5 shows the diversity of the microbial activities along the stages. As expected, the respiration rates of heterotrophic biomass (X_H) and ammonia oxidation bacteria (AOB) in stage 1 and stage 3 were substantially higher than that in the other stages. This was in accordance with the distribution of the influent loading (Fig. 1 and Table 1) and the mass reduction in each stage (Fig. 4). The striking feature revealed in Fig. 5 was the diversity of nitrifying activities in different stages. Respiration rate of AOB was 12 times of NOB in stage 1. It (OUR_{AOB}/OUR_{NOB}) decreased to 0.75 in stage 2 and 3, and increased again to 1.5 in stage 4. From the stoichiometry of ammonia oxidization (nitritation) (Eq. 1) and nitrite oxidization (nitratation) (Eq. 2) reactions (Wiesmann et al., 2007), OUR_{AOB}/OUR_{NOB} should be at 3 if the rates of these two processes are equal. If this ratio is above 3, nitritation should be faster than nitratation and vice versa. Based on the OUR_{AOB}/OUR_{NOB}

of 12 and the neglectable accumulation of NO_X^--N in stage 1, it could be inferred that most of the nitrite was denitrified once produced, i.e. partial nitrification and SND via nitrite was the main nitrogen removal mechanism in stage 1. This result further highlighted the significance of enhancing NH_4^+-N reduction in stage 1 since denitrification via nitrite can save carbon source by 40% (Turk & Mavinic, 1987). Accordingly, the nitrogen removal mechanism in the stages 2 to 4 was mainly nitrification and denitrification via nitrate, which could be concluded by the increased NOB activity (Fig. 5) and buildup of nitrate (Fig. 2e).

[Fig. 5]

$$NH_4^+ + 1.5\,O_2 \rightarrow NO_2^- + H_2O + 2H^+ \qquad (1)$$

$$NO_2^- + 0.5\,O_2 \rightarrow NO_3^- \qquad (2)$$

3.5 Theoretical approach on optimizing step-feeding TFCWs

Although satisfactory TN removal performance was achieved with step-feeding in this study, the best scheme (scheme D) was still not optimized for maximum N removal. The optimal step-feeding setup should be configured to ensure that the total Kjeldahl nitrogen (TKN) is completely nitrified in the aerobic stage(s) to provide maximum oxidized N. Proper distribution of the influent into the anoxic stage(s) is required to meet the carbon requirement for full denitrification (Tang et al., 2007). From the cyclic profiles (Fig. 3d), it can be seen that substantial NH_4^+-N still remained in the outflow of stage 2, which limited the available oxidized N in the side input stage (stage 3). Furthermore, the side input stage was not strictly anoxic, which limited denitrification. Hence, scheme D can be further optimized in configuration as proposed and shown in Fig. 6. Initially, an adequate aerobic stage (A1) is formed with down flow stages (S_1 to S_i) to completely oxidize TKN in the primary feed. The number of these stages depends on the nitrogen loading rate. In addition, bed resting time can be further adjusted to 3 hrs with T_C of 6 hrs. Following A1, an effective anoxic stage (S_{i+1}) can be formed by adopting up flow pattern. The effectiveness of bed resting and flow pattern on controlling the redox state has been justified in section 3.3. At the end, another down flow stage (S_{i+2}) is setup, which serves as the second aerobic stage (A2) to remove the NH_4^+-N introduced by the flow distribution. This optimal setup can make the most efficient utilization of the influent carbon source and thus can achieve maximum TN removal.

Obviously, the flow distribution fraction (*f*) (See Fig. 6) is the most important parameter in step-feeding CWs. However, there is still a lack of mathematical framework to determine it. Wastewater was distributed evenly into each feed point in the early step-feeding CWs design (Dialynas et al., 2002; Sundaravadivel and Vigneswaran, 2001; USEPA, 1988). Recently, some efforts have been made to investigate the optimal flow distribution fraction by comparing the treatment performance with different distribution ratios (Stefanakis et al., 2011). These empirical methods are insufficient to ensure maximum removal efficiency.

In fact, *f* is to provide sufficient BCOD (biodegradable COD) for complete denitrification in the anoxic stage (S_{i+1}) and can be presented by the inequality of Eq. (3), in which $f \times \mathrm{BCOD}_{in}$ represents the available carbon source introduced by the flow distribution and $(1\text{-}f) \times \mathrm{TKN}_{in}$ is the amount of nitrified N generated in the aerobic stages (S_1-S_i). The constant k is a stoichiometric ratio, which is the amount of BCOD required to reduce 1 unit mass of NO_X^--N into nitrogen gas (Tang et al., 2007). In the current study, the effect of SND should be taken into account since significant amount of NO_X^--N is denitrified in A1 as evidenced in Fig. 3. Therefore, a reduction factor (β) is introduced (Eq. 4). Rearranging Eq. (4) yields the relationship between f and the influent BCOD/TKN ratio (Eq. 5). The maximum N removal efficiency can be achieved when f is minimized (Eq. 6). Eq. 6 reveals that the optimal influent distribution ratio for maximum nitrogen removal is a function of the influent BCOD/TKN ratio, rather than a fixed value. Therefore, the optimal distribution fraction should be adjusted regularly according to the influent wastewater characteristics in step-feeding strategy.

$$f \times BCOD_{in} \geq k \times (1-f) \times TKN_{in} \qquad (3)$$

$$f \times BCOD_{in} \geq k \times \beta \times (1-f) \times TKN_{in} \qquad (4)$$

$$f \geq \frac{k\beta}{\frac{BCOD_{in}}{TKN_{in}} + k\beta} \qquad (5)$$

$$f_{min} = \frac{k\beta}{\frac{BCOD_{in}}{TKN_{in}} + k\beta} \qquad (6)$$

4. Conclusions

This study provides ample evidence on step-feeding strategy in AlS-TFCWs to achieve enhanced TN removal. With the best scheme D, average TN removal of 83% can be achieved, which is a substantial improvement of TN removal in TFCWs, making it be able to deliver tertiary effluent under nitrogen loading rate of 19.1 g N/m^2 d and hydraulic loading rate of 0.29 m^3/m^2 d. Sufficient bed resting time is demonstrated to be the key factor to maintain the effective nitrification while up flow pattern and delayed input of the side stream(s) are the key factors for a better denitrification.

Acknowledgements

Authors gratefully acknowledge financial support received from the Irish state Department of Agriculture, Fisheries and Food under the Research Stimulus Fund (project no. RSF 07-529). The UCD farm, Lyons Estate, Newcastle, Co. Dublin and Mr. Michael Hegarthy are sincerely thanked for their kind support.

References

[1] Artan, N., Orhon, D. 2005. *Mechanisms and design of sequencing batch reactors for nutrient removal*. IWA Publishers, London, UK.

[2] Babatunde, A.O., Zhao, Y.Q., Burke, A.M., Morris, M.A., Hanrahan, J.P. 2009. Characterization of aluminium-based water treatment residual for potential phosphorus removal in engineered wetlands. *Environ Pollut*, **157**(10), 2830-2836.

[3] Babatunde, A.O., Zhao, Y.Q., Zhao, X.H. 2010. Alum sludge-based constructed wetland system for enhanced removal of P and OM from wastewater: Concept, design and performance analysis. *Bioresource Technol*, **101**(16), 6576-6579.

[4] Chan, S.Y., Tsang, Y.F., Chua, H. 2008. Domestic wastewater treatment using tidal-flow cinder bed with Cyperus alternifolius. *Aquat Ecosyst Health*, **11**(2), 206-211.

[5] Clesceri, L.S., Greenberg, A.E., Eaton, A.D. 1998. Standard methods for the examination of water and wastewater. 20th ed, American Public Health Association. Washington, DC.

[6] Dialynas, G., Kefalakis, N., Dialynas, M., Angelakis, A. 2002. Performance of an innovative FWS constructed wetland in Crete, Greece. *Water Sci Technol*, **46**(4-5), 355-360.

[7] Fillos, J., Diyamandoglu, V., Carrio, L.A., Robinson, L. 1996. Full-scale evaluation of biological nitrogen removal in the step-feed activated sludge process. *Water Environ Res*, **68**(2), 132-142.

[8] Fujii, S. 1996. Theoretical analysis on nitrogen removal of the step-feed anoxic-oxic activated sludge process and its application for the optimal operation. *Water Sci Technol*, **34**(1-2), 459-466.

[9] Ginestet, P., Audic, J.M., Urbain, V., Block, J.C. 1998. Estimation of nitrifying bacterial activities by measuring oxygen uptake in the presence of the metabolic inhibitors allylthiourea and azide. *Appl Environ Microb*, **64**(6), 2266-2268.

[10] House, C.H., Bergmann, B.A., Stomp, A.M., Frederick, D.J. 1999. Combining constructed wetlands and aquatic and soil filters for reclamation and reuse of water. *Ecol Eng*, **12**(1-2), 27-38.

[11] Hu, Y.S., Kumar, J.L.G., Akintunde, A.O., Zhao, X.H., Zhao, Y.Q. 2011. Effects of livestock wastewater variety and disinfectants on the performance of constructed wetlands in organic matters and nitrogen removal. *Environ Sci Pollut R*, **18**(8), 1414-1421.

[12] Liang, H.W., Gao, M., Liu, J.X., Wei, Y.S., Guo, X.S. 2010. A novel integrated step-feed biofilm process for the treatment of decentralized domestic wastewater in rural areas of China. *J Environ Sci-China*, **22**(3), 321-327.

[13] Münch, E.V., Lant, P., Keller, J. 1996. Simultaneous nitrification and denitrification in bench-scale sequencing batch reactors. *Water Res*, **30**(2), 277-284.

[14] Pochana, K., Keller, J. 1999. Study of factors affecting simultaneous nitrification and denitrification (SND). *Water Sci Technol*, **39**(6), 61-68.

[15] Puig, S., Vives, M.T., Corominas, L., Balaguer, M.D., Colprim, J. 2004. Wastewater nitrogen removal in SBRs, applying a step-feed strategy: from lab-scale to pilot-plant operation. *Water Sci Technol*, **50**(10), 89-96.

[16] Reed, S.C., Brown, D.S. 1992. Constructed Wetland Design: The First Generation. *Water Environ Res*, **64**(6), 776-781.

[17] Sato, C., Schnoor, J.L., Mcdonald, D.B., Huey, J. 1985. Test Medium for the Growth of Nitrosomonas-Europaea. *Appl Environ Microb*, **49**(5), 1101-1107.

[18] Stefanakis, A.I., Akratos, C.S., Tsihrintzis, V.A. 2011. Effect of wastewater step-feeding on removal efficiency of pilot-scale horizontal subsurface flow constructed wetlands. *Ecol Eng*, **37**(3), 431-443.

[19] Stottmeister, U., Wießner, A., Kuschk, P., Kappelmeyer, U., Kästner, M., Bederski, O., Müller, R.A., Moormann, H. 2003. Effects of plants and microorganisms in constructed wetlands for wastewater treatment. *Biotechnol Adv*, **22**(1-2), 93-117.

[20] Sun, G., Gray, K.R., Biddlestone, A.J. 1999a. Treatment of agricultural wastewater in a pilot-scale tidal flow reed bed system. *Environ Technol*, **20**(2), 233-237.

[21] Sun, G., Gray, K.R., Biddlestone, A.J., Cooper, D.J. 1999b. Treatment of agricultural wastewater in a combined tidal flow-downflow reed bed system. *Water Sci Technol*, **40**(3), 139-146.

[22] Sun, G., Zhao, Y.Q., Allen, S. 2005. Enhanced removal of organic matter and ammoniacal-nitrogen in a column experiment of tidal flow constructed wetland system. *J Biotechnol*, **115**(2), 189-197.

[23] Sun, G., Zhao, Y., Allen, S., Cooper, D. 2006. Generating "tide" in pilot-scale constructed wetlands to enhance agricultural wastewater treatment. *Eng Life Sci*, **6**(6), 560-565.

[24] Sundaravadivel, M., Vigneswaran, S. 2001. Constructed wetlands for wastewater treatment. *Crit Rev Env Sci Tec*, **31**(4), 351-409.

[25] Tang, C.-C., Kuo, J., Weiss, J.S. 2007. Maximum Nitrogen Removal in the Step-Feed Activated Sludge Process. *Water Environ Res*, **79**(4), 367-374.

[26] Turk, O., Mavinic, D.S. 1987. Benefits of Using Selective-Inhibition to Remove Nitrogen from Highly Nitrogenous Wastes. *Environ Technol Lett*, **8**(9), 419-426.

[27] USEPA. 1988. Design Manual – Constructed Wetlands and Aquatic Plant Systems for Municipal Wastewater Treatment, Office of Research and Development, Center for Environmental Research Information. Cincinnati, Ohio, pp. 47-55.

[28] Vymazal, J. 2011. Constructed Wetlands for Wastewater Treatment: Five Decades of Experience. *Environ Sci Technol*, **45**(1), 61-69.

[29] Wiesmann, U., Choi, S., Dombrowski, E.-M. 2007. Fundamentals of Biological Wastewater Treatment, Wiley–VCH Weinheim, Germany, pp. 228.

[30] Yang, Y., Zhao, Y.Q., Wang, S.P., Guo, X.C., Ren, Y.X., Wang, L., Wang, X.C. 2011. A promising approach of reject water treatment using a tidal flow constructed wetland system employing alum sludge as main substrate. *Water Sci Technol*, **63**(10), 2367-2373.

[31] Zhao, Y.Q., Babatunde, A.O., Hu, Y.S., Kumar, J.L.G., Zhao, X.H. 2011. Pilot field-scale demonstration of a novel alum sludge-based constructed wetland system for enhanced wastewater treatment. *Process Biochem*, **46**(1), 278-283.

[32] Zhao, Y.Q., Sun, G., Allen, S.J. 2004a. Purification capacity of a highly loaded laboratory scale tidal flow reed bed system with effluent recirculation. *Sci Total Environ*, **330**(1-3), 1-8.

[33] Zhao, Y.Q., Sun, G., Lafferty, C., Allen, S.J. 2004b. Optimising the performance of a lab-scale tidal flow reed bed system treating agricultural wastewater. *Water Sci Technol*, **50**(8), 65-72.

[34] Zhao, Y.Q., Zhao, X.H., Babatunde, A.O. 2009. Use of dewatered alum sludge as main substrate in treatment reed bed receiving agricultural wastewater: Long-term trial. *Bioresource Technol*, **100**(2), 644-648.

Tables:

Table 1 Summary of the tested step-feeding schemes

Schemes (Operational days)	Input points	Distribution ratio (%)	Cycle time (T_C, hrs)	Wet/Dry (min)	Main flow pattern	HLR (m^3/m^2 d)	HRT (hrs)
A (26-99)	Stage 1, 3	80:20	4	230:10	Down flow	0.44	36
B (130-164)	Stage 1, 3, 4	85:10:5	6	240:120	Down flow	0.29	57
C (191-289)	Stage 1, 3	90:10	6	240:120	Stage 3 up flow	0.29	57
D (293-383)	Stage 1, 3	80:20	6	240:120	Stage 3 up flow	0.29	57

HLR: hydraulic loading rate; HRT: hydraulic retention time (based on total reactor volume)

Table 2 Influent wastewater characteristics (Mean ± SD) and average loading rates

	Scheme A (26-99 days)	Scheme B (130-164 days)	Scheme C (191-289 days)	Scheme D (293-383 days)
COD (mg/L)	478 ± 120	481 ± 50	495 ± 51	482 ± 63
TN (mg/L)	55 ± 11	59 ± 4	61 ± 3	66 ± 6
NH_4^+-N (mg/L)	48 ± 13	53 ± 6	57 ± 6	55 ± 8
TP (mg/L)	9 ± 2	11 ± 3	12 ± 3	10 ± 2
SS (mg/L)	159 ± 60	319 ± 121	256 ± 67	112 ± 46
pH	7.2 ± 0.3	7.6 ± 0.1	7.4 ± 0.4	7.5 ±0.3
COD/TN	8.9 ± 2.5	8.1 ±0.5	8.2 ± 1.0	7.3 ± 1.1
OLR (kg COD/m^2 d)	0.21	0.13	0.14	0.14
NLR(g N/m^2 d)	24.2	17.1	17.7	19.1
PLR(g P/m^2 d)	4.0	3.5	3.5	2.9

OLR: organic loading rate; NLR: nitrogen loading rate; PLR: phosphorus loading rate

Table 3 Mass flux of NH_4^+-N reduction ($\varphi_{NH4,Re.}$) and NO_X^--N accumulation ($\varphi_{NOX,Acc.}$) in each stage (mg/d)

	Stage	Scheme A (S1:S3=0.8:0.2)	Scheme B (S1:S3:S4=0.85:0.1:0.05)	Scheme C (S1:S3=0.9:0.1)	Scheme D (S1:S3=0.8:0.2)
$\varphi_{NH4,Re.}$	1	$Q\times0.8\times(NH_{4,in}-NH_{4,S1})$	$Q\times0.85\times(NH_{4,in}-NH_{4,S1})$	$Q\times0.9\times(NH_{4,in}-NH_{4,S1})$	$Q\times0.8\times(NH_{4,in}-NH_{4,S1})$
	2	$Q\times0.8\times(NH_{4,S1}-NH_{4,S2})$	$Q\times0.85\times(NH_{4,S1}-NH_{4,S2})$	$Q\times0.9\times(NH_{4,S1}-NH_{4,S2})$	$Q\times0.8\times(NH_{4,S1}-NH_{4,S2})$
	3	$Q\times(0.8\times NH_{4,S2}+0.2\times NH_{4,in}-NH_{4,S3})$	$Q\times(0.85\times NH_{4,S2}+0.1\times NH_{4,in}-0.95\times NH_{4,S3})$	$Q\times(0.9\times NH_{4,S2}+0.1\times NH_{4,in}-NH_{4,S3})$	$Q\times(0.8\times NH_{4,S2}+0.2\times NH_{4,in}-NH_{4,S3})$
	4	$Q\times(NH_{4,S3}-NH_{4,S4})$	$Q\times(0.95\times NH_{4,S3}+0.05\times NH_{4,in}-NH_{4,S4})$	$Q\times(NH_{4,S3}-NH_{4,S4})$	$Q\times(NH_{4,S3}-NH_{4,S4})$
$\varphi_{NOX,Acc.}$	1	$Q\times0.8\times(NO_{X,S1}-NO_{X,in})$	$Q\times0.85\times(NO_{X,S1}-NO_{X,in})$	$Q\times0.9\times(NO_{X,S1}-NO_{X,in})$	$Q\times0.8\times(NO_{X,S1}-NO_{X,in})$
	2	$Q\times0.8\times(NO_{X,S2}-NO_{X,S1})$	$Q\times0.85\times(NO_{X,S2}-NO_{X,S1})$	$Q\times0.9\times(NO_{X,S2}-NO_{X,S1})$	$Q\times0.8\times(NO_{X,S2}-NO_{X,S1})$
	3	$Q\times(NO_{X,S3}-0.8\times NO_{X,S2}-0.2\times NO_{X,in})$	$Q\times(0.95\times NO_{X,S3}-0.85\times NO_{X,S2}-0.1\times NO_{X,in})$	$Q\times(NO_{X,S3}-0.9\times NO_{X,S2}-0.1\times NO_{X,in})$	$Q\times(NO_{X,S3}-0.8\times NO_{X,S2}-0.2\times NO_{X,in})$
	4	$Q\times(NO_{X,S4}-NO_{X,S3})$	$Q\times(NO_{X,S4}-0.95\times NO_{X,S3}-0.05\times NO_{X,in})$	$Q\times(NO_{X,S4}-NO_{X,S3})$	$Q\times(NO_{X,S4}-NO_{X,S3})$

Q: flow rate, L/d; Scheme A, Q=12; Scheme B-D, Q=8.

$NH_{4,\,in}$, $NO_{X,\,in}$: influent NH_4^+-N and NO_X^--N, mg/L.

$NH_{4,Si}$, $NO_{X,Si}$: effluent NH_4^+-N and NO_X^--N of each stage, mg/L; i=1-4.

Table 4 Multiple comparisons between different step-feeding schemes on treatment performance

Dependent Variable	(I) Group	(J) Group	Mean Difference (I-J)	Std. Error	Sig.	95% Confidence Interval Lower Bound	Upper Bound
SS	A	B	-1.71286	1.82781	0.934	-7.2767	3.8509
		C	0.42092	1.82270	1.000	-4.6839	5.5257
		D	-0.59143	1.99610	1.000	-6.1372	4.9544
	B	A	1.71286	1.82781	0.934	-3.8509	7.2767
		C	2.13378	2.01155	0.886	-3.8318	8.0994
		D	1.12143	2.16991	0.997	-5.1612	7.4041
	C	A	-.42092	1.82270	1.000	-5.5257	4.6839
		B	-2.13378	2.01155	0.886	-8.0994	3.8318
		D	-1.01235	2.16561	0.998	-7.0311	5.0064
	D	A	0.59143	1.99610	1.000	-4.9544	6.1372
		B	-1.12143	2.16991	0.997	-7.4041	5.1612
		C	1.01235	2.16561	0.998	-5.0064	7.0311
COD	A	B	-1.18238	2.72351	0.999	-9.1330	6.7682
		C	8.70384*	2.71379	0.017	1.1494	16.2583
		D	4.10165	2.31444	0.416	-2.3801	10.5834
	B	A	1.18238	2.72351	0.999	-6.7682	9.1330
		C	9.88622*	2.61390	0.009	2.1314	17.6410
		D	5.28403	2.19646	0.189	-1.7019	12.2699
	C	A	-8.70384*	2.71379	0.017	-16.2583	-1.1494
		B	-9.88622*	2.61390	0.009	-17.6410	-2.1314
		D	-4.60219	2.18440	0.237	-10.7821	1.5777
	D	A	-4.10165	2.31444	0.416	-10.5834	2.3801
		B	-5.28403	2.19646	0.189	-12.2699	1.7019
		C	4.60219	2.18440	0.237	-1.5777	10.7821

BOD_5	A	B	-5.35473	3.67887	0.667	-16.6073	5.8978
		C	-3.73273	6.07075	0.992	-22.4098	14.9443
		D	-10.06473	3.18950	0.056	-20.3442	0.2147
	B	A	5.35473	3.67887	0.667	-5.8978	16.6073
		C	1.62200	5.53299	1.000	-16.4619	19.7059
		D	-4.71000	1.98315	0.342	-13.3882	3.9682
	C	A	3.73273	6.07075	0.992	-14.9443	22.4098
		B	-1.62200	5.53299	1.000	-19.7059	16.4619
		D	-6.33200	5.22042	0.835	-24.3042	11.6402
	D	A	10.06473	3.18950	0.056	-0.2147	20.3442
		B	4.71000	1.98315	0.342	-3.9682	13.3882
		C	6.33200	5.22042	0.835	-11.6402	24.3042
TP	A	B	0.53095	0.73337	0.983	-2.1081	3.1700
		C	1.10919	0.80418	0.706	-1.2596	3.4780
		D	2.67413*	0.49692	0.000	1.2740	4.0742
	B	A	-0.53095	0.73337	0.983	-3.1700	2.1081
		C	0.57824	1.04654	0.995	-2.4929	3.6494
		D	2.14318	0.83395	0.143	-0.5035	4.7899
	C	A	-1.10919	0.80418	0.706	-3.4780	1.2596
		B	-.57824	1.04654	0.995	-3.6494	2.4929
		D	1.56495	0.89685	0.442	-0.9857	4.1156
	D	A	-2.67413*	0.49692	0.000	-4.0742	-1.2740
		B	-2.14318	0.83395	0.143	-4.7899	0.5035
		C	-1.56495	0.89685	0.442	-4.1156	0.9857
NH_4^+-N	A	B	-9.62619*	1.58211	0.000	-14.1389	-5.1135
		C	-5.12308*	1.76776	0.038	-10.0587	-0.1875
		D	-8.69918*	1.46436	0.000	-12.9496	-4.4488
	B	A	9.62619*	1.58211	0.000	5.1135	14.1389
		C	4.50311*	1.20209	0.007	1.0297	7.9765
		D	0.92701	0.68149	0.762	-1.4717	3.3257

	C	A	5.12308*	1.76776	0.038	0.1875	10.0587
		B	-4.50311*	1.20209	0.007	-7.9765	-1.0297
		D	-3.57610*	1.04227	0.018	-6.6614	-0.4908
	D	A	8.69918*	1.46436	0.000	4.4488	12.9496
		B	-0.92701	0.68149	0.762	-3.3257	1.4717
		C	3.57610*	1.04227	0.018	0.4908	6.6614
TN	A	B	-11.13571*	2.80963	0.004	-19.2001	-3.0713
		C	-8.93454	3.39585	0.074	-18.4195	0.5504
		D	-22.22253*	2.40484	0.000	-29.0674	-15.3776
	B	A	11.13571*	2.80963	0.004	3.0713	19.2001
		C	2.20118	3.06595	0.980	-6.6621	11.0645
		D	-11.08682*	1.91089	0.001	-17.4111	-4.7625
	C	A	8.93454	3.39585	0.074	-0.5504	18.4195
		B	-2.20118	3.06595	0.980	-11.0645	6.6621
		D	-13.28799*	2.69986	0.001	-21.1740	-5.4020
	D	A	22.22253*	2.40484	0.000	15.3776	29.0674
		B	11.08682*	1.91089	0.001	4.7625	17.4111
		C	13.28799*	2.69986	0.001	5.4020	21.1740

*. The mean difference is significant at the 0.05 level.

Figure captions:

Fig. 1 Schematic representation of the 4 stages step-feeding AlS-TFCWs. Step-feeding scheme (A) Two steps (Feed 1 80%, Feed 2 20%), down flow; (B) Three steps (Feed 1 85%, Feed 2 10%, Feed 3 5%), down flow; (C) Two steps (Feed 1 90%, Feed 2 10%), stage 3 up flow; (D) Two steps (Feed 1 80%, Feed 2 20%), stage 3 up flow.

Fig. 2 Overall performance of the step-feeding AlS-TFCWs for each step-feeding scheme: (a) SS removal; (b) COD removal; (c) TP removal; (d) Nitrification; (e) effluent NO_2^--N and NO_3^--N; (f) TN removal.

Fig. 3 Cyclic nitrogen profiles under different step-feeding schemes (Mean value for each scheme).

Fig. 4 N mass balances and DO distribution: (a) Removal percentage of influent NH_4^+-N loading in each stage; (b) Mass NH_4^+-N reduction in each stage; (c) Mass NO_X^--N accumulation in each stage; (d) Vertical initial DO distribution after down flow /up flow pulse-feeding (2 l in 10 min, error bars denote S.D., n=3).

Fig. 5 Microbial activities of individual stages at the end of scheme D (error bars denote S.D., n=2).

Fig. 6 Proposed optimal configuration for step-feeding AlS-TFCWs

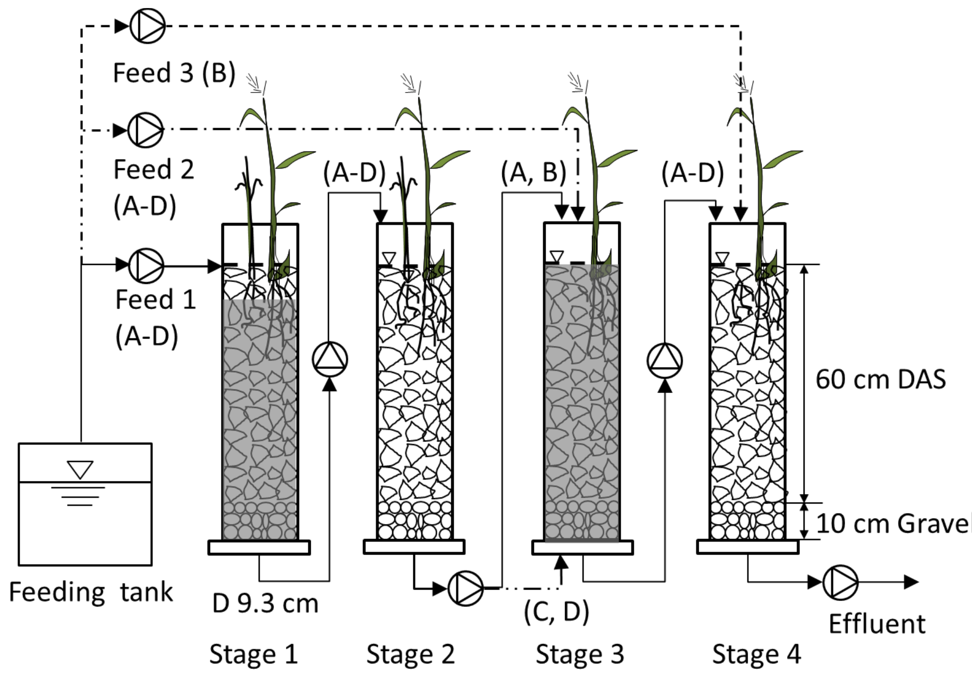
Feed 3 (B)
Feed 2
(A-D)
Feed 1
(A-D)
(A-D)
(A, B)
(A-D)
60 cm DAS
10 cm Gravel
Feeding tank
D 9.3 cm
(C, D)
Effluent
Stage 1
Stage 2
Stage 3
Stage 4

Fig. 1

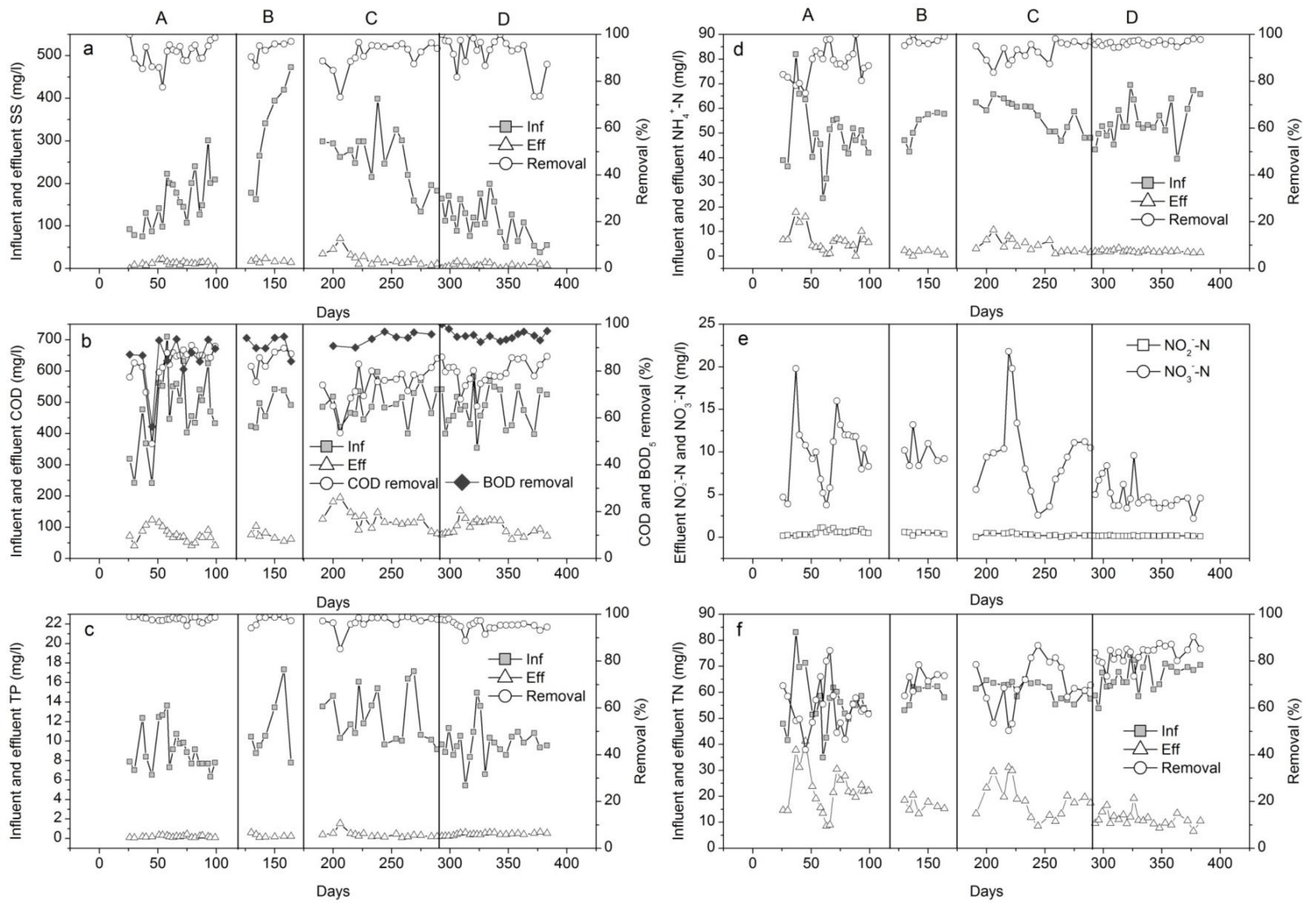

A
B
C
D
a
Influent and effluent SS (mg/l)
Removal (%)
Inf
Eff
Removal
Days
b
Influent and effluent COD (mg/l)
COD and BOD5 removal (%)
COD removal
BOD removal
c
Influent and effluent TP (mg/l)
d
Influent and effluent NH4+-N (mg/l)
e
Effluent NO2−-N and NO3−-N (mg/l)
NO2−-N
NO3−-N
f
Influent and effluent TN (mg/l)

Fig. 2

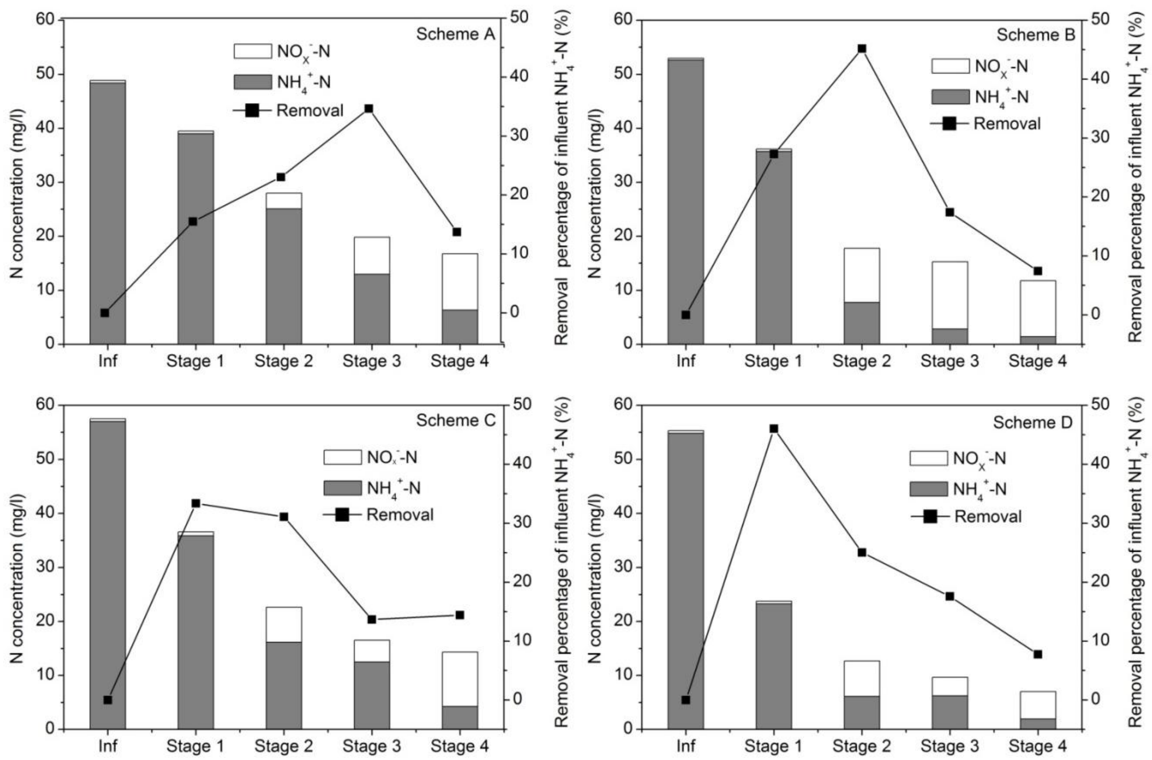
Scheme A
Scheme B
Scheme C
Scheme D
NO_X^--N
NH_4^+-N
Removal
N concentration (mg/l)
Removal percentage of influent NH_4^+-N (%)
Inf
Stage 1
Stage 2
Stage 3
Stage 4

Fig. 3

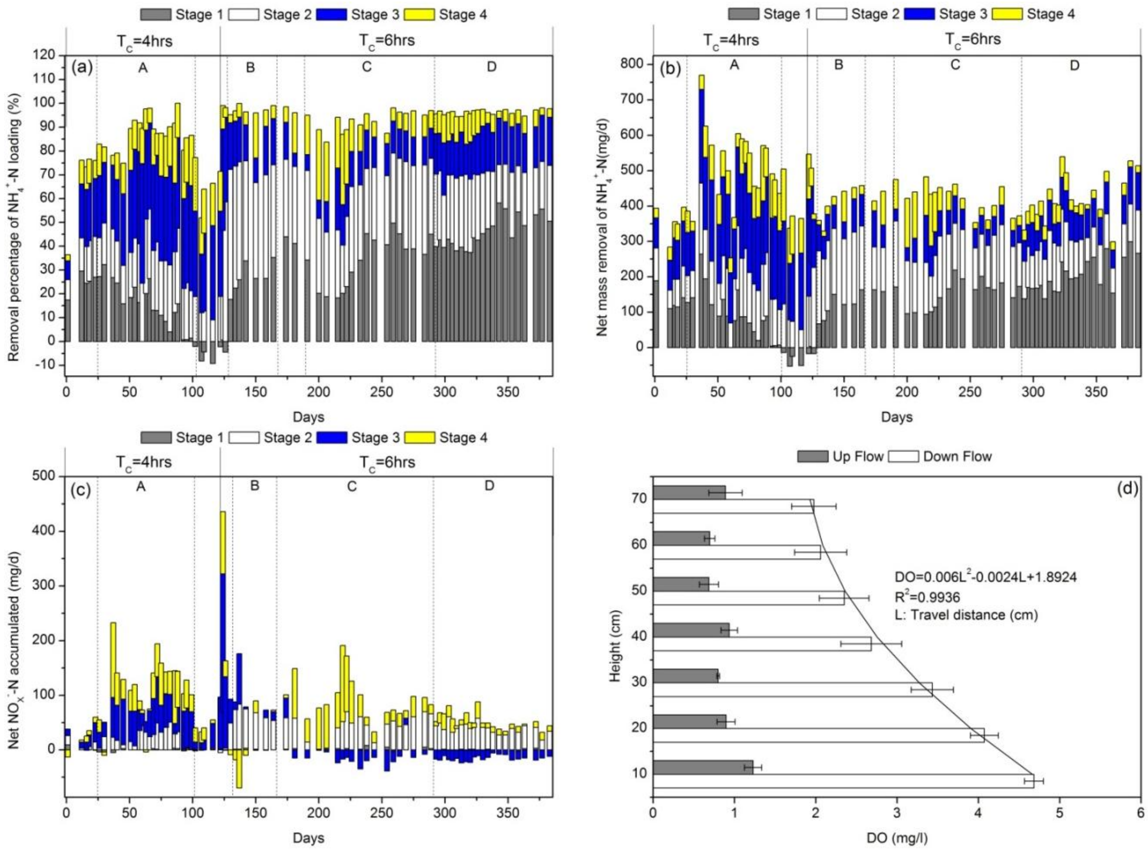

Stage 1
Stage 2
Stage 3
Stage 4
T_C=4hrs
T_C=6hrs
(a)
A
B
C
D
Removal percentage of NH_4^+-N loading (%)
Days
(b)
Net mass removal of NH_4^+-N(mg/d)
(c)
Net NO_X^--N accumulated (mg/d)
Up Flow
Down Flow
(d)
DO=0.006L^2-0.0024L+1.8924
R^2=0.9936
L: Travel distance (cm)
Height (cm)
DO (mg/l)

Fig. 4

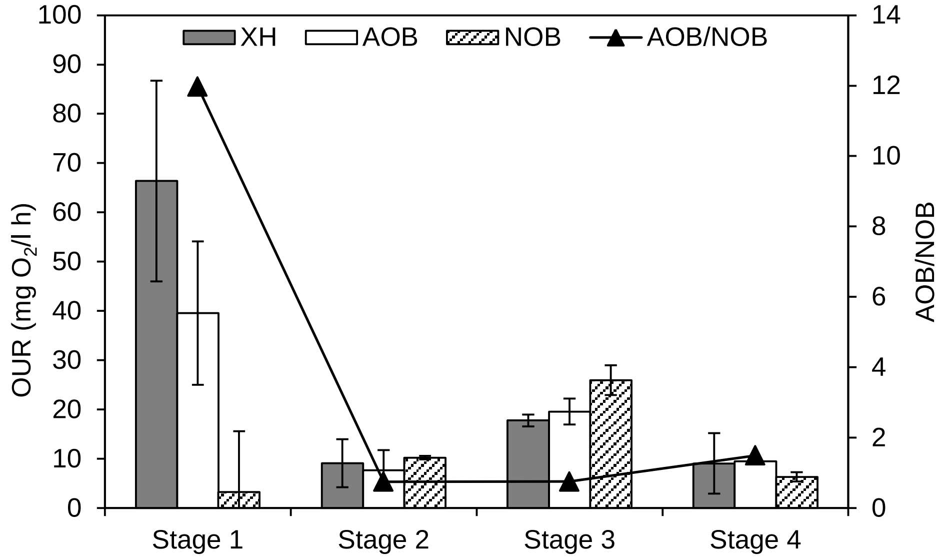

XH
AOB
NOB
AOB/NOB
OUR (mg O2/l h)
AOB/NOB
100
90
80
70
60
50
40
30
20
10
0
14
12
10
8
6
4
2
0
Stage 1
Stage 2
Stage 3
Stage 4

Fig. 5

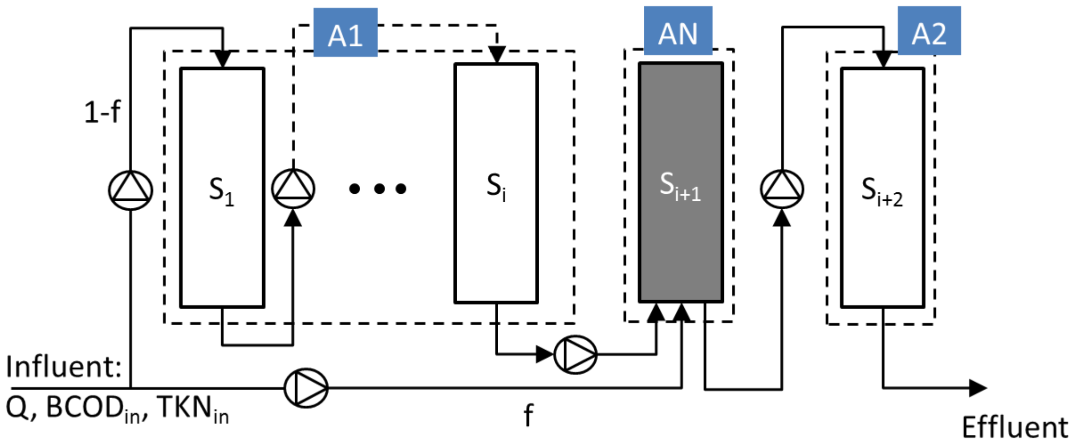

Fig. 6